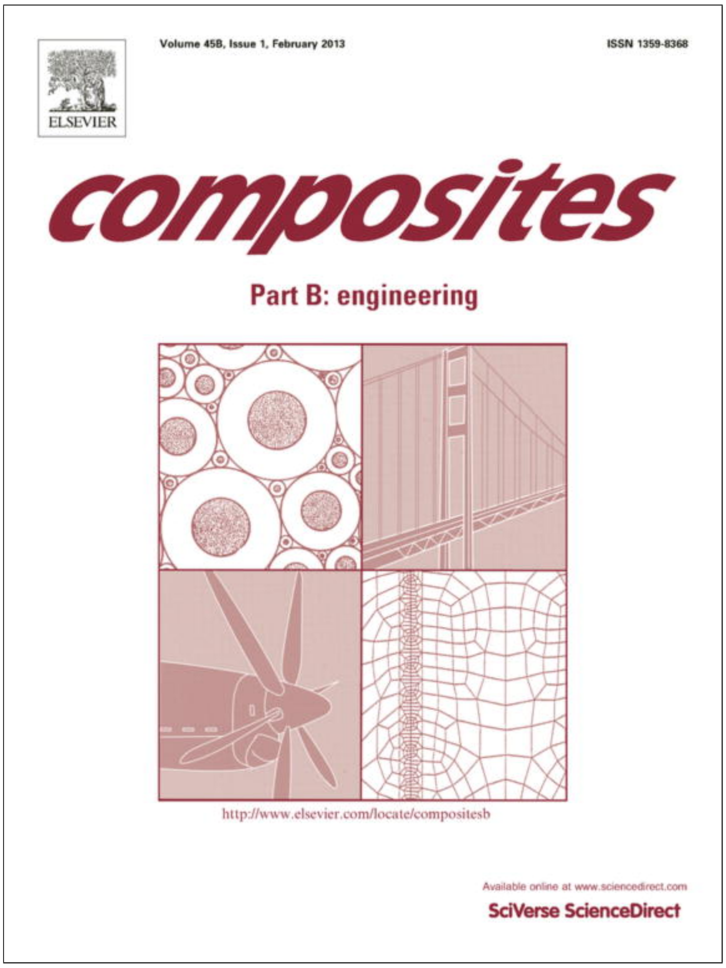
ELSEVIER
Volume 45B, Issue 1, February 2013
ISSN 1359-8368
composites
Part B: engineering
http://www.elsevier.com/locate/compositesb
Available online at www.sciencedirect.com
SciVerse ScienceDirect

Composites: Part B 45 (2013) 845–851

Contents lists available at SciVerse ScienceDirect

Composites: Part B

journal homepage: www.elsevier.com/locate/compositesb

# Indentation stress in multi-layer delaminated thin films induced by a microwedge indenter

MingHao Zhao [a,b,*], HaiTao Liu [b], CuiYing Fan [a], Ernian Pan [a], Tong-Yi Zhang [c]

[a] The School of Mechanical Engineering, Zhengzhou University, Zhengzhou, Henan 450001, China
[b] Department of Engineering Mechanics, Zhengzhou University, Zhengzhou, Henan 450001, China
[c] Department of Mechanical Engineering, Hong Kong University of Science and Technology, Clear Water Bay, Kowloon, Hong Kong, China

ARTICLE INFO

*Article history:*
Received 18 March 2012
Received in revised form 20 July 2012
Accepted 6 August 2012
Available online 23 August 2012

*Keywords:*
A. Thin films
B. Residual/internal stress
C. Analytical modeling
D. Mechanical testing
E. Microwedge indentation test

ABSTRACT

Indentation stresses in single- and multi-layer delaminated thin films made of elastic–perfectly plastic materials in microwedge indentation delamination tests are analyzed via finite element calculations with different wedge angles and other geometrical and mechanical parameters. Based on the formula for a single-layer thin film under indentation loading [Zhao et al. J Mater Res 2009;24:1943] and by introducing the equivalent material parameters, we developed simple analytical formulae for the loading indentation stress (as well as the energy release rate) in each layer of the multi-layer thin film, in terms of the residual stress, elastic modulus, Poisson's ratio, yielding strength, and thickness of each layer. Our analytical solution is validated by the finite element calculations and should be useful to thin-film delamination tests.


## 1. Introduction

With the wide use of thin films in micro/nanoelectromechanical systems (MEMS/NEMS), testing and characterizing mechanical properties of film/substrate systems, such as the film residual stress and interfacial fracture toughness between adjacent layers, become critically important to MEMS/NEMS. As such, various experimental methods/techniques have been developed, such as the microcantilever beam test, microbridge test, bulge test, and micro/nanoindentation tests [1], among which the microwedge indentation test is one of the most important and convenient mechanical testing methods [2,3] due to its relatively simple analysis process involved. Various effects in the microwedge indentation test have been studied including the effect of the compliant substrate on the film deformation [4–6], the effect of the indentation-induced impression or notch [6] and the size effect of the indented film [7] on the buckling behaviors of the delaminated film.

When the indenter tip penetrates into a tested film/substrate sample, a compressive stress field, called indentation stress, is generated in the film, which is essential to indentation delamination [8]. Studying a single-layer film, Zhao et al. [9] defined two kinds of indentation stresses, namely the loading and unloading indentation stresses, which occur during loading and unloading process, respectively, in the indentation test. By fitting the numerical results, Zhao et al. [9] derived the following expression for the loading indentation stress $\sigma_{IL}$:

$$\begin{cases} \sigma_{IL}/E_p = 0.2650\left(\frac{E}{E_0}\right)^{-0.1184}\left(\frac{t}{a}\right)^{0.7035}\left(\frac{h}{t}\right)^{2}\tan^{1.2656}\varphi, & h/t < h_c/t, \\ \sigma_{IL}/\sigma_s = 1.1483, & h/t \geqslant h_c/t \end{cases} \tag{1}$$

in which $t$ is the film thickness, $a$ half of the delamination length, $h$ the indentation depth, and $E_p = E/(1-\nu^2)$ is the plane-strain Young's modulus, with $E$ and $\nu$ being, respectively, the Young's modulus and Poisson's ratio of the thin film; $E_0 = 1$ GPa is a normalization factor, $\sigma_s$ the yielding strength, $2\varphi$ the wedge angle, and $h_c$ is the critical depth, which, for plastic deformation, is given by

$$(h_c/t)^2 = 3.8527\frac{\sigma_s}{E}\left(\frac{E}{E_0}\right)^{0.1184}\left(\frac{t}{a}\right)^{-0.7035}\tan^{-1.2656}\varphi. \tag{2}$$

Indentation on the thin-film system could be also investigated experimentally. For example, for the multi-layer thin-film substrate system, Bagchi et al. [10,11] developed a method to measure the interfacial fracture resistance of ductile films on substrates by depositing a second super-layer of material which has a large intrinsic stress. Kriese et al. [12,13], by following Marshall and Evans's work [8] on single-layer indentation delamination test (with a cone indenter), extended the test to the general multi-layer

* Corresponding author. Address: The School of Mechanical Engineering, Zhengzhou University, No. 100 Science Road, Zhengzhou, Henan Province 450001, China. Tel.: +86 371 67781832; fax: +86 371 67781786.
*E-mail addresses:* memhzhao@zzu.edu.cn, memhzhao@sina.com (M. Zhao).

1359-8368/$ - see front matter 
http://dx.doi.org/10.1016/j.compositesb.2012.08.010

case, and further discussed the experimental results for thin films made of copper, tungsten, and chromium. An et al. [14] carried out the experiment on the TiN/SiN$_x$ thin film over the Si substrate.

While indentation on multi-layer thin films was experimentally investigated in [10–14], the corresponding analytical study is rare. This is because that in deriving the analytical solution for the indentation delamination in a multi-layer thin-film/substrate system, one must first deal with the following three important issues:

One issue is to include the film residual stress, which is generally induced during film deposition, in the indentation stress formulas. In indentation test, the indentation stress is induced due to the plastic deformation or damage of the indented film. In the linear approach, superposition is usually applied to take the film residual stress into account. However, indentation-induced delamination is a complicated nonlinear process. It could be problematic to directly apply the linear superposition there. The second important issue is to obtain the indentation stress in multi-layer thin film/substrate systems, in which each layer has its own thickness, elastic and plastic properties. To develop a reliable formula similar to Eq. (1) for the indentation stress in each layer of multi-layer films is the other objective of the present study. The last issue is to calculate the energy release rate and phase angle of the cracked tip between the multi-layer thin film and the substrate.

Aiming at resolving these three important issues, we follow the previous approach [9] to numerically solve the problem with a large range of parameters and then fit the numerical data into the proposed dimensionless formulas of the indentation stress. As in [9], zero friction is assumed between the indenter and the film surface (we actually validated this assumption by comparing the results from both friction and zero-friction cases). The paper is organized as follows: In Section 2, we derive an analytical expression for the indentation stress at yielding. In Section 3, we analyze the indentation stress in a single-layer film with residual stress and study the effect of the film residual stress. In Sections 4 and 5, bi-layer and multi-layer films are, respectively, analyzed and new empirical formulas of the indentation stresses are derived. Using the stress field, the energy release rate is calculated in Section 6 for a bi-layer film system. Finally, conclusions are drawn in Section 7.

## 2. Indentation stress at yielding

Fig. 1 shows the finite element model of the film system. In this model, the length of the wedge indenter tip is larger than the film width. A coordinate system is attached such that the $(x, z) \equiv (x_1, x_3)$ plane coincides with the interface, where delamination occurs. For a thin-film structure, the plane-stress holds along the film thickness direction and the plane-strain is used along the beam width direction. In this case, if the stress field is only induced by indentation, then the three principle stresses can be expressed in terms of the indentation stress $\sigma_{IL}$ as

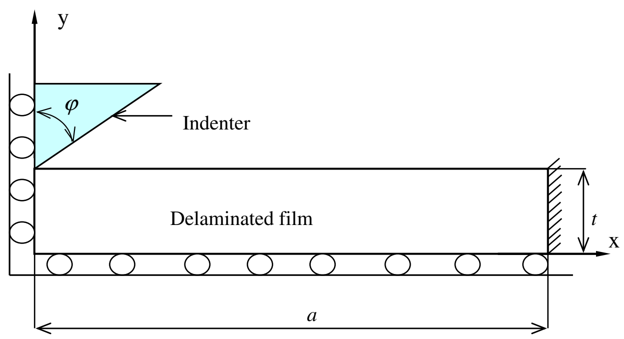


**Fig. 1.** A single-layer film indented by a microwedge indenter.

$$\sigma_1 = \sigma_{IL}, \quad \sigma_2 = 0, \quad \sigma_3 = \nu\sigma_{IL}, \tag{3}$$

where $\sigma_1$, $\sigma_2$ and $\sigma_3$ are the three principle stresses along, respectively, the $x_1$-, $x_2$-, and $x_3$-directions.

Substituting Eq. (3) into the von Mises yielding criterion

$$(\sigma_1 - \sigma_2)^2 + (\sigma_2 - \sigma_3)^2 + (\sigma_3 - \sigma_1)^2 = 2\sigma_s^2, \tag{4}$$

gives

$$\sigma_{IL} = \sigma_s \Big/ \sqrt{1 - \nu + \nu^2}. \tag{5}$$

Eq. (5) shows how the indentation stress varies with Poisson's ratio of the film. When $\nu = 0.3333$, $\sigma_{IL} = 1.1339\sigma_s$, which is approximately the same as the previous calculation result, with a relative error of about 1.25% as compared to the second equation in Eq. (1).

## 3. Indentation stress in a single-layer film with residual stress

The two-dimensional finite element method (FEM) is employed to calculate numerically the stress in the delaminated film during indentation loading and unloading, with the commercial code ANSYS. Due to the symmetry of the problem, only half of the FEM model is shown in Fig. 1. The film beam is fixed at both ends and is simply supported on its lower surface. The microwedge indenter is assumed to be rigid and the film is assumed to be elastic–perfectly plastic following the stress–strain relationship

$$\begin{cases} \sigma = \varepsilon E + \sigma_r, & |\varepsilon| < (\sigma_s - \text{sign } \varepsilon\, \sigma_r)/E, \\ \sigma = \sigma_s \text{sign } \varepsilon, & |\varepsilon| \geqslant (\sigma_s - \text{sign } \varepsilon\, \sigma_r)/E, \end{cases} \tag{6}$$

where $\sigma$ is the total stress, $\varepsilon$ the strain, $\sigma_r$ the initial stress or the residual stress, and "sign" is the sign function. The von Mises yielding criterion is used in the analysis. The geometric and material parameters used in the FEM are given below

$$\begin{cases} \varphi = 60^\circ, 75^\circ \\ h/t = 0.01667\text{—}0.8, \\ a/t = 10,\ 15,\ 25, \\ \sigma_s = 100\text{—}800\ (\text{MPa}), \\ E = 50\text{—}480\ (\text{GPa}), \quad \nu = 0.3333, \\ \sigma_r = 0\text{—}\pm 400\ (\text{MPa}), \end{cases} \tag{7}$$

where $\sigma_r$ again is the residual stress along the $x$-direction (or the longitudinal direction of the film). The PLANE82 elements are used in the FEM as shown in Fig. 2. The FEM results show that the stress field in the film is almost uniform except for a small region under the indenter tip and near the fixed end. This uniform stress is defined as the indentation stress, which is investigated systematically below.

Fig. 3 plots the indentation stress in the film versus the indentation depth for different yielding strengths. These curves exhibit two regions. In the first region, the indentation stress is independent of the yielding strength and nonlinearly changes with the indentation depth, which can be fitted by a parabola passing point $(0, \sigma_r)$. In the second region, the indentation stress is independent of the indentation depth, forming a plateau after the normalized indentation depth exceeds a critical value $h_c/t$ which depends strongly on the yielding strength. From the FEM results, the indentation stress in the delaminated film in the loading stage for the parabola part of the curve can be calculated by Eq. (1) except for replacing $\sigma_{IL}$ by $\sigma_{IL}$ - $\sigma_r$, i.e.,

$$\begin{cases} (\sigma_{IL} - \sigma_r)/E_P = 0.2650\left(\frac{E}{E_0}\right)^{-0.1184}\left(\frac{t}{a}\right)^{0.7035}\left(\frac{h}{t}\right)^2 \tan^{1.2656}\varphi, & h/t < h_c/t, \\ \sigma_{IL}/\sigma_s = (1 - \nu + \nu^2)^{-0.5}, & h/t \geqslant h_c/t, \end{cases} \tag{8}$$

from which the critical indentation depth is found to be

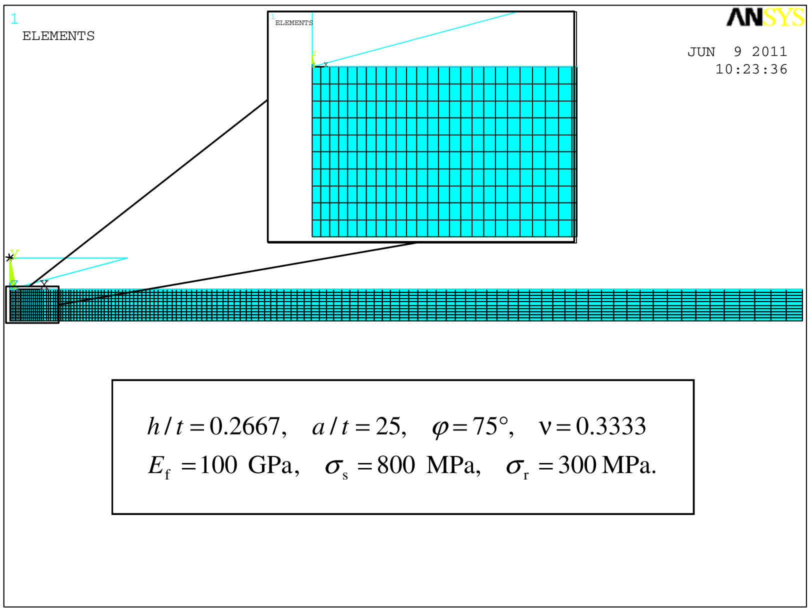


**Fig. 2.** Finite element mesh of the indented single-layer film.

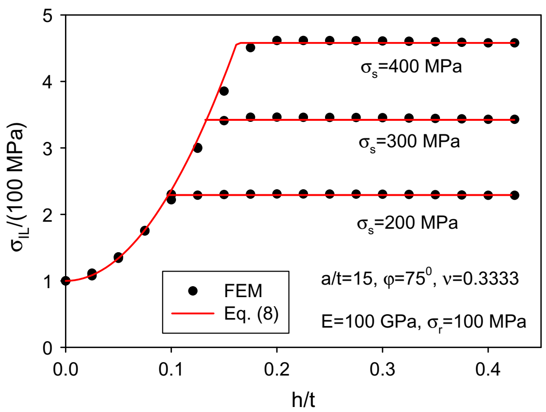


**Fig. 3.** Indentation stress versus indentation depth in the single-layer film with different yielding strengths.

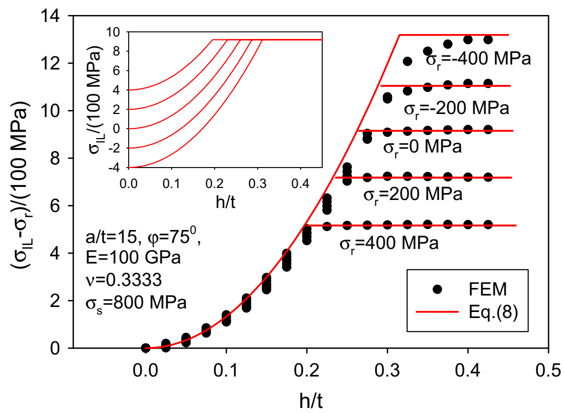


**Fig. 4.** Film stress (indentation stress minus residual stress) versus indentation depth in the single-layer film with different residual stresses.

$$(h_c/t)^2 = 3.7736\frac{(1-\nu+\nu^2)^{-0.5}\sigma_s-\sigma_r}{E_p}\left(\frac{E}{E_0}\right)^{0.1184}\left(\frac{t}{a}\right)^{-0.7035} \times \tan^{-1.2656}\varphi. \tag{9}$$

As expected, the indentation stress equals the residual stress in the film $\sigma_{IL} = \sigma_r$ when the indentation depth $h = 0$. Eqs. (8) and (9) are the corresponding extensions of Eqs. (1) and (2). If the residual stress is zero, as expected, Eqs. (8) and (9) are then reduced, respectively, to Eqs. (1) and (2). Although the relationship between the indentation stress and indentation depth is nonlinear, the contribution of the residual stress to the indentation stress follows the simple superposition.

Fig. 4 plots the film stress (indentation stress minus the residual stress) versus the indentation depth for different residual stresses, with the inserted figure being the variation of the indentation stress. The results demonstrate that, in the first part of the curve (the parabola part) the stress difference is independent of the residual stress and that the results from Eq. (8) agree well with those from FEM. Also for comparison, the inserted figure shows the indentation stress versus the indentation depth. It is observed that while the parabola part is different under different residual stresses, the horizontal lines are independent of the residual stress in the film.

## 4. Indentation stress in a bi-layer film with residual stresses

Similarly, the FEM is employed to analyze the stress in the delaminated bi-layer film, with the model being schematically shown in Fig. 5. The boundary conditions are the same as those used for the single-layer film. The two layers are perfectly bonded along the interface as widely used in the existing theoretical models [10–14]. Parameters used in the FEM are given below

$$\begin{cases} \varphi = 60^\circ, 75^\circ \\ h/t = 0.01667\text{–}0.8, \\ a/t = 10,\ 15,\ 25, \\ \sigma_{s1},\ \sigma_{s2} = 100\text{–}900\ (\text{MPa}), \\ E_1,\ E_2 = 50\text{–}480\ (\text{GPa}), \\ \nu_1,\ \nu_2 = 0.1\text{–}0.4, \\ \sigma_{r1},\ \sigma_{r2} = 0\text{–}\pm 400\ (\text{MPa}), \end{cases} \tag{10}$$

with the subscripts "1" and "2" denoting the properties in the first and second layers, respectively. Fig. 6a and b shows, respectively,

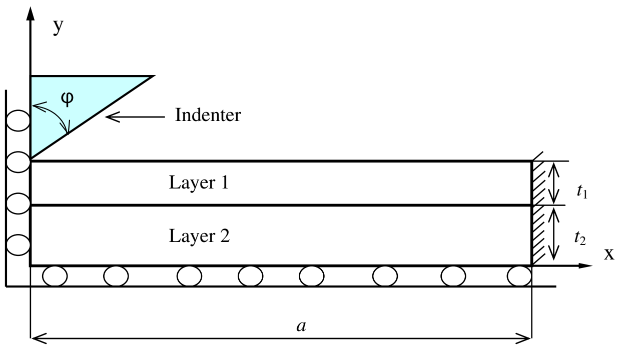


**Fig. 5.** A bi-layer film indented by a microwedge indenter.

the finite element mesh and the corresponding stress distribution in the delaminated bi-layer film. Again, similar to the single-layer case, the stress in each layer is almost uniform except for a small region (with size being about the film thickness) under the indenter tip and near the clamped end of the film (Fig. 6b).

The FEM results for the indentation stress versus the indentation depth in the two layers without residual stress are shown in Fig. 7 (the open squares and solid circles). It is observed that the indentation stresses in the two layers satisfy the following relation:

$$\sigma_{IL1}/E_{p1} = \sigma_{IL2}/E_{p2} = \sigma_{ILe}/E_{pe}, \tag{11}$$

with

$$E_{pe} = E_e/(1 - \nu_e^2), \tag{12}$$

where the added subscript "e" denotes the corresponding equivalent parameters (e.g., equivalent Young's modulus $E_e$ and Poisson's ratio $\nu_e$), which are defined as

$$\frac{t}{E_e} = \frac{t_1}{E_1} + \frac{t_2}{E_2}, \quad \frac{t}{\nu_e} = \frac{t_1}{\nu_1} + \frac{t_2}{\nu_2}, \quad t = t_1 + t_2. \tag{13}$$

The FEM results in Fig. 6a and b show that the stress in each layer is approximately constant and can be expressed by

$$\begin{cases} \sigma_{ILi}/E_{Pi} = 0.2650\left(\frac{E_e}{E_0}\right)^{-0.1184}\left(\frac{t}{a}\right)^{0.7035}\left(\frac{h}{t}\right)^2 \tan^{1.2656}\varphi, & h/t < h_{ci}/t, \\ \sigma_{ILi}/\sigma_{si} = (1 - \nu_i + \nu_i^2)^{-0.5}, & h/t \geqslant h_{ci}/t, \end{cases} \tag{14}$$

where $i = 1, 2$, denotes the layer number. The critical indentation depth in each layer ($i = 1, 2$) is found to be

$$(h_{ci}/t)^2 = 3.7736\frac{(1 - \nu_i + \nu_i^2)^{-0.5}\sigma_{si}}{E_{pi}}\left(\frac{E_e}{E_0}\right)^{0.1184}\left(\frac{t}{a}\right)^{-0.7035} \times \tan^{-1.2656}\varphi. \tag{15}$$

The equations for bi-layer films are similar to those for the single-layer film, as indicated by comparing Eqs. (14) and (15) with Eqs. (1) and (2) for fixed $\nu = 0.3333$. The indentation stress vs. indentation depth in each layer is also shown in Fig. 7 (the dashed and solid lines), illustrating clearly that the indentation stresses based on Eq.

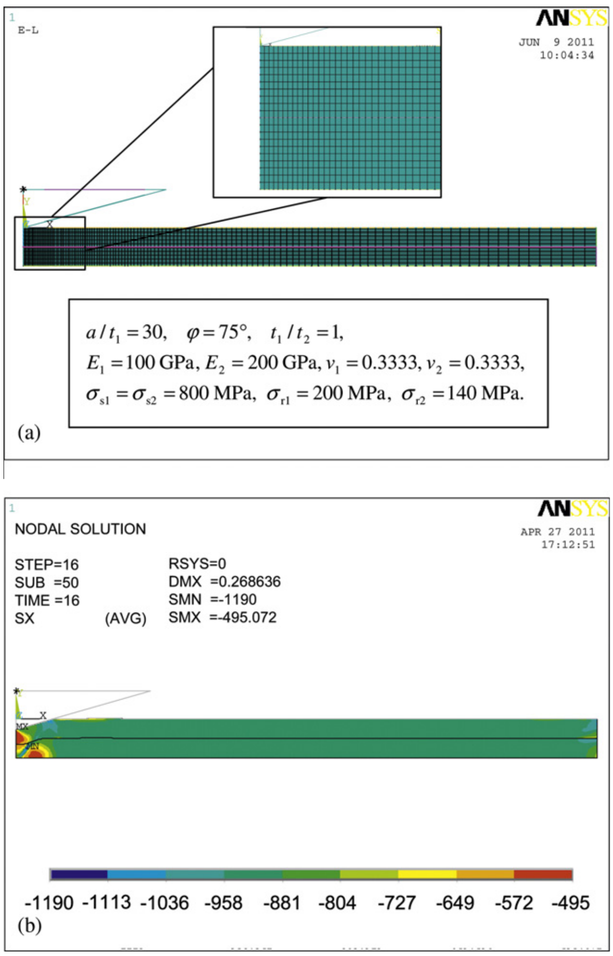


**Fig. 6.** (a) Finite element mesh and (b) the corresponding stress distribution via FEM in the indented bi-layer film.

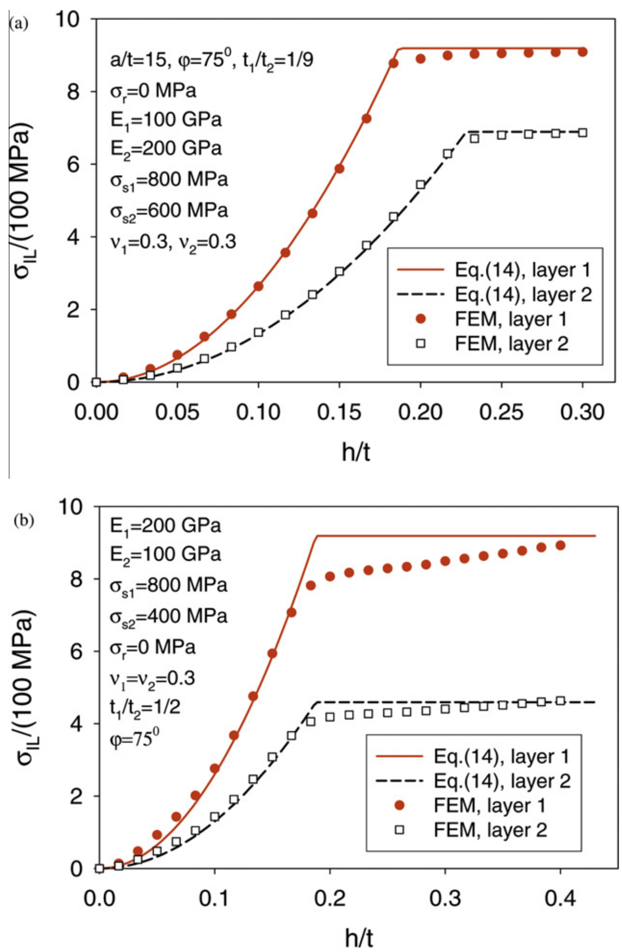


**Fig. 7.** Indentation stress versus indentation depth in the indented bi-layer film. (a and b) Represent results with different material and geometrical parameters.

(14) is in good agreement with the FEM results for different material and geometrical parameters.

Similarly, taking the residual stress into consideration, the film stress in each layer can be simply calculated by

$$\begin{cases} (\sigma_{\mathrm{IL}i} - \sigma_{\mathrm{r}i})/E_{\mathrm{P}i} = 0.2650\left(\frac{E_e}{E_0}\right)^{-0.1184}\left(\frac{t}{a}\right)^{0.7035}\left(\frac{h}{t}\right)^{2}\tan^{1.2656}\varphi, & h/t < h_{\mathrm{c}i}/t, \\ \sigma_{\mathrm{IL}i}/\sigma_{si} = (1 - \nu_i + \nu_i^2)^{-0.5}, & h/t \geqslant h_{\mathrm{c}i}/t, \end{cases} \tag{16}$$

where

$$(h_{\mathrm{c}i}/t)^2 = 3.7736\frac{(1-\nu_i+\nu_i^2)^{-0.5}\sigma_{si} - \sigma_{\mathrm{r}i}}{E_{\mathrm{p}i}}\left(\frac{E_\mathrm{e}}{E_0}\right)^{0.1184}\left(\frac{t}{a}\right)^{-0.7035} \times \tan^{-1.2656}\varphi. \tag{17}$$

Fig. 8 shows the indentation stresses in both layers versus the indentation depth calculated using Eq. (16), which are again very close to those by the FEM.

## 5. Indentation stress in a multi-layer film with residual stresses

Inspired by the results for bi-layer films, we conducted further FEM calculations to analyze the indentation stresses in multi-layer films with different geometric and material parameters. Our FEM results show that the indentation stress in each layer of a multi-layer film can still be calculated by Eqs. (14) and (16) with $i = 1, 2, \ldots, n$. Similar to Eq. (13), the equivalent elastic parameters, $E_\mathrm{e}$, $\nu_\mathrm{e}$ and $E_\mathrm{pe}$, can be calculated by the following equations:

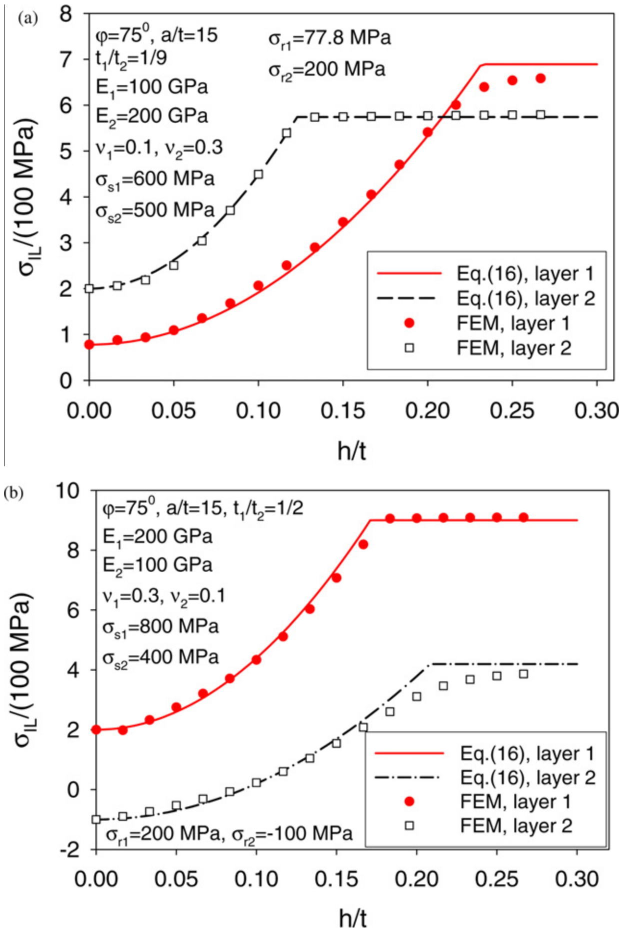


**Fig. 8.** Indentation stress versus indentation depth in the indented bi-layer film with residual stresses. (a) For positive residual stress in both layers and (b) for positive (negative) residual stress in layer 1 (2).

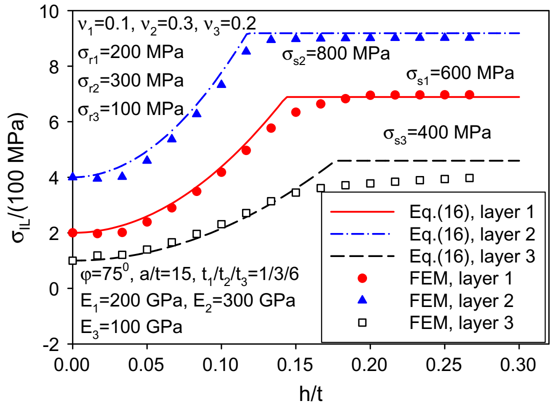


**Fig. 9.** Indentation stress versus indentation depth in a tri-layer film with residual stresses.

$$\begin{aligned} &\tfrac{t}{E_e} = \tfrac{t_1}{E_1} + \tfrac{t_2}{E_2} + \cdots + \tfrac{t_n}{E_n}, \\ &\tfrac{t}{\nu_e} = \tfrac{t_1}{\nu_1} + \tfrac{t_2}{\nu_2} + \cdots + \tfrac{t_n}{\nu_n}, \\ &E_{\mathrm{pe}} = E_\mathrm{e}/(1-\nu_\mathrm{e}^2), \\ &t = t_1 + t_2 + \cdots + t_n, \end{aligned} \tag{18}$$

where $n$ is the total layer number of the multi-layer film.

Fig. 9 shows the indentation stresses vs. indentation depth in each layer of a tri-layer film without residual stress, whilst Fig. 10 plots the indentation stresses vs. indentation depth in each layer of a five-layer film with residual stresses. Both figures show very good fitting of the empirical formulae as compared to the FEM results.

## 6. Energy release rate in a bi-layer film

With the indentation stress in the film system, one can also calculate the corresponding energy release rate. As an example, we consider the energy release rate for a bi-layer film with zero residual stress. Fig. 11 illustrates a bi-layer film (with thickness $t_1$ and $t_2$) over a substrate of finite thickness $H$ with an interface crack between the second layer and substrate, under forces (horizontal forces $P_\mathrm{i}$ and moment $M_\mathrm{s}$) due to the indentation stress. Now we let the crack tip extend a distance $dL$ along the interface, then the change of the external work $dW$ by the forces and the change of the internal strain energy $dU$ is, respectively,

$$dW = t_1\sigma_{\mathrm{IL}1}\varepsilon\delta dL + t_2\sigma_{\mathrm{IL}2}\varepsilon\delta dL + \frac{P_s^2}{E_sH}\delta dL + \frac{12}{E_s}\frac{M_s^2}{H^3}\delta dL, \tag{19}$$

$$dU = \frac{t_1\sigma_{\mathrm{IL}1}^2}{2E_1}\delta dL + \frac{t_2\sigma_{\mathrm{IL}2}^2}{2E_2}\delta dL + \frac{P_s^2}{2E_sH}\delta dL + \frac{6}{E_s}\frac{M_s^2}{H^3}\delta dL, \tag{20}$$

where $\varepsilon$ is the uniform strain in the bi-layer film and $\delta$ is the width of the film. Then, the energy release rate $G$ is

$$\begin{aligned} G &= \frac{dW}{dA} - \frac{dU}{dA} \\ &= t_1\sigma_{\mathrm{IL}1}\varepsilon + t_2\sigma_{\mathrm{IL}2}\varepsilon - \frac{t_1\sigma_{\mathrm{IL}1}^2}{2E_1} - \frac{t_2\sigma_{\mathrm{IL}2}^2}{2E_2} + \frac{P_s^2}{2E_sH} + \frac{6}{E_s}\frac{M_s^2}{H^3}. \end{aligned} \tag{21}$$

For the substrate with an infinite thickness, $H \to \infty$, and Eq. (21) is thus reduced to

$$G = t_1\sigma_{\mathrm{IL}1}\varepsilon + t_2\sigma_{\mathrm{IL}2}\varepsilon - \frac{t_1\sigma_{\mathrm{IL}1}^2}{2E_1} - \frac{t_2\sigma_{\mathrm{IL}2}^2}{2E_2}. \tag{22}$$

Fig. 12 shows the normalized energy release rate $G$ vs. the indentation depth in the bi-layer film-substrate system of Fig. 11 (with $H$ = infinity) with zero residual stress (with $E_0$ = 1 GPa being

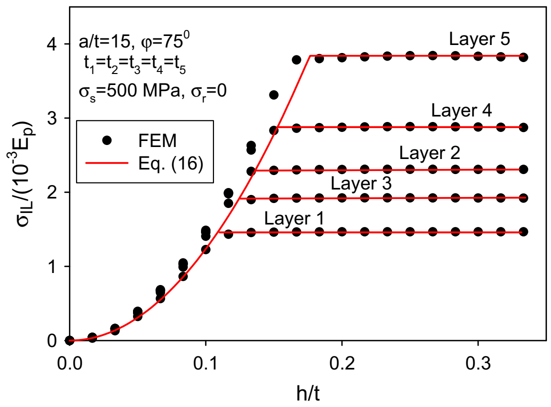


**Fig. 10.** Indentation stress versus indentation depth in a five-layer film. The Young's moduli and Poisson's ratios in the five layers are: $E_1 = 350$ GPa, $\nu_1 = 0.3333$; $E_2 = 250$ GPa, $\nu_2 = 0.4444$; $E_3 = 300$ GPa, $\nu_3 = 0.2222$; $E_4 = 200$ GPa, $\nu_4 = 0.1111$; and $E_5 = 150$ GPa, $\nu_5 = 0.3333$.

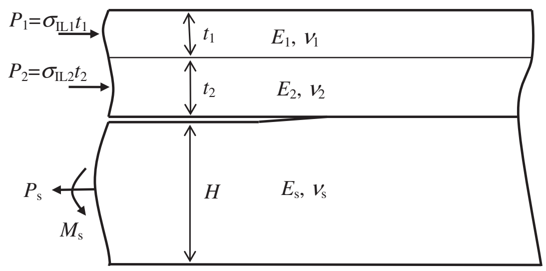


**Fig. 11.** An interfacial crack between the bi-layer film and substrate, under forces (horizontal forces $P_i$ and moment $M_s$) due to the indentation stress in the system.

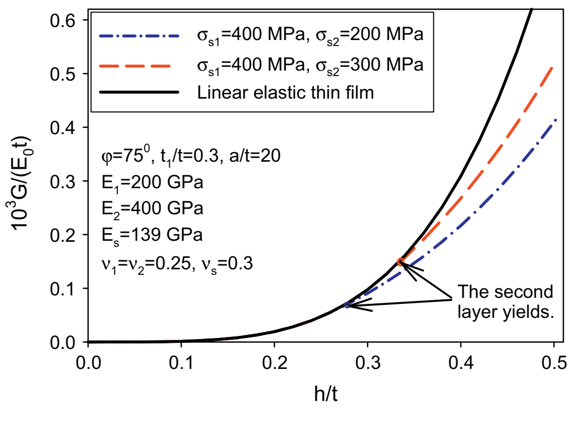


**Fig. 12.** Normalized energy release rate vs. indentation depth in a bi-layer film/substrate system as shown in Fig. 11 with $H$ = infinity.

the normalization factor). The parameters used for the calculation are also listed in the figure. The energy release rate for the corresponding linear elastic films is also shown for comparison. It is observed clearly that, under different yielding strengths in the second layer (with fixed $\sigma_{s1} = 400$ MPa in the first layer), the curve of the energy release rate will depart from the corresponding linear elastic curve at different normalized indentation depth – a smaller departure point of the indentation depth corresponds to a smaller yield strength.

We point out that Kriese et al. [12] discussed the phase angles in multi-layered systems. They stated [12] that if there were only indentation-induced stresses, the test geometry would be directly analogous to the wedge indentation as studied in this paper, and hence the phase angle should initially be equal to ω and decrease on buckling (with the values of parameter ω being tabulated in [15]).

## 7. Conclusion and discussion

The two-dimensional finite element calculations are conducted to simulate the microwedge indentation test on the multi-layer thin-film system with elastic–perfectly plastic properties (without buckling). The following important conclusions can be drawn from our analysis:

1. The stress in the indented film can be obtained simply by superposition of the residual stress and the stress induced by indentation, although the relationship between the indentation stress and indentation depth is nonlinear, thereby indicating that the influence of the residual stress can be easily assessed in the indentation delamination test. The corresponding energy release rate in a bi-layer film-substrate system is also derived and numerical results are further given to illustrate its dependence on the indentation depth.
2. With equivalent elastic Young's moduli and Poisson's ratios, the proposed simple analytical formulae, as functions of the film residual stress, elastic modulus, Poisson's ratio and the yielding strength of each layer, describe accurately the indentation stress in each layer of an indented multi-layer film of elastic–perfectly plastic materials.

We finally remark that there are still some related works to be done in the future. First, in our paper, we considered material yielding but not buckling of the film; thus, film buckling in yielding stage should be an important but complicated issue. Second, in this paper, we did not calculate the phase angle in multi-layer thin film which would be a challenging topic for future investigation.

## Acknowledgements

The work was supported by the National Natural Science Foundation of China (Nos. 11272290, 11102186), Program for Innovative Research Team (in Science and Technology) in University of Henan Province (No. 2010IRTSTHN013), and the Bairen Program in Henan Province.

## References

[1] Volinsky AA, Moody NR, Gerberich WW. Interfacial toughness measurements for thin films on substrates. Acta Mater 2002;50:441–66.
[2] de Boer MP, Gerberich WW. Microwedge indentation of the thin film fine line – I. Mechanics. Acta Mater 1996;44:3169–75.
[3] de Boer MP, Gerberich WW. Microwedge indentation of the thin film fine line – II. Experiment. Acta Mater 1996;44:3177–87.
[4] Cotterell B, Chen Z. Buckling and cracking of thin films on compliant substrate under compression. Int J Fract 2000;104:169–79.
[5] Yu HH, Hutchinson JW. Influence of substrate compliance on buckling delamination of thin films. Int J Fract 2002;113:39–55.
[6] Zhao MH, Yang F, Zhang TY. Delamination buckling in the microwedge indentation of a thin film on an elastically deformable substrate. Mech Mater 2007;39:881–92.
[7] Liu T, Hai M, Zhao MH. Delaminating buckling model based on nonlocal Timoshenko beam. Eng Fract Mech 2008;75:4909–19.
[8] Marshall DB, Evans AG. Measurement of adherence of residually stressed thin films by indentation. I. Mechanics of interface delamination. J Appl Phys 1984;56:2632–8.
[9] Zhao MH, Yao LP, Zhang TY. Stress analysis of microwedge indentation-induced delamination. J Mater Res 2009;24:1943–9.
[10] Bagchi A, Lucas GE, Suo Z, Evans AG. A new procedure for measuring the decohesion energy for thin ductile films on substrates. J Mater Res 1994;9:1734–41.

[11] Bagchi A, Evans AG. Measurements of the debond energy for thin metallization lines on dielectrics. Thin Solid Films 1996;286:203–12.
[12] Kriese MD, Gerberich WW, Moody NR. Quantitative adhesion measures of multilayer films: Part I. Indentation mechanics. J Mater Res 1999;14:3007–18.
[13] Kriese MD, Gerberich WW, Moody NR. Quantitative adhesion measures of multilayer films: Part II. Indentation of W/Cu, W/W, Cr/W. J Mater Res 1999;14:3019–26.
[14] An T, Wen M, Hu CQ, Tian HW, Zheng WT. Interfacial fracture for TiN/$SiN_x$ nano-multilayer coatings on Si(111) characterized by nanoindentation experiments. Mater Sci Eng A 2008;494:324–8.
[15] Suo Z, Hutchinson JW. Interface crack between two elastic layers. Int J Fract 1990;43:1–18.